

**SUPPLEMENTARY MATERIALS:
TARGET PREDICTION AND A STATISTICAL SAMPLING ALGORITHM
FOR RNA-RNA INTERACTION**

FENIX W.D. HUANG¹, JING QIN¹, CHRISTIAN M. REIDYS^{1,2}, AND PETER F. STADLER^{3,4,5,6}

1. PRELIMINARIES

1.1. **Definitions.** Given two RNA sequences R and S (e.g. an antisense RNA and its target) with N and M vertices, we index the vertices such that R_1 is the 5' end of R and S_1 denotes the 3' end of S . The edges of R and S represent the intramolecular base pairs. A *pre-structure*, $G(R, S, I)$, is a graph with the following properties:

- (1) R, S are secondary structures (each nucleotide being paired with at most one other nucleotide via hydrogen bonds, without internal pseudoknots);
- (2) I is a set of arcs of the form $R_i S_j$ without pseudoknots, i.e., if $R_{i_1} S_{j_1}, R_{i_2} S_{j_2} \in I$ where $i_1 < i_2$, then $j_1 < j_2$ holds.

An arc is called *exterior* if it is of the form $R_i S_j$ and *interior*, otherwise. Let G be a graph and V be a subset of G -vertices. The (*induced*) *subgraph* of G induced by V has vertex set V and contains all G -edges having both incident vertices in V . In particular, we use $S[i, j]$ to denote the subgraph of the pre-structure $G(R, S, I)$ induced by $\{S_i, S_{i+1}, \dots, S_j\}$, where $S[i, i] = S_i$ and $S[i, i-1] = \emptyset$. In absence of interactions a pre-structure is a pair of induced secondary structures on R and S , which we will refer to as a pair of *segments*. A segment $S[i_1, j_1]$ is called maximal if there is no segment, $S[i, j]$ strictly containing $S[i_1, j_1]$.

An interior arc $R_{i_1} R_{j_1}$ is an *R-ancestor* of the exterior arc $R_i S_j$ if $i_1 < i < j_1$. Analogously, $S_{i_2} S_{j_2}$ is an *S-ancestor* of $R_i S_j$ if $i_2 < j < j_2$. The sets of *R-ancestors* and *S-ancestors* of $R_i S_j$

Date: Sep, 2009.

are denoted by $A_R(R_i S_j)$ and $A_S(R_i S_j)$, respectively. We will also refer to $R_i S_j$ as a descendant of $R_{i_1} R_{j_1}$ and $S_{i_2} S_{j_2}$ in this situation. The R - and S -ancestors of $R_i S_j$ with minimum arc-length are referred to as R - and S -parents, see Fig. 1, (A). Finally, we call $R_{i_1} R_{j_1}$ and $S_{i_2} S_{j_2}$ dependent if they have a common descendant and independent, otherwise.

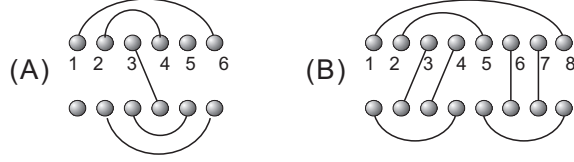


FIGURE 1. (A) Ancestors and parents: for the exterior arc $R_3 S_4$, we have the following ancestor sets $A_R(R_3 S_4) = \{R_1 R_6, R_2 R_4\}$ and $A_S(R_3 S_4) = \{S_2 S_6, S_3 S_5\}$. In particular, $R_2 R_4$ and $S_3 S_5$ are the R -parent and S -parent respectively. (B) Subsumed and equivalent arcs: $R_1 R_8$ subsumes $S_1 S_4$ and $S_5 S_8$. Furthermore, $R_2 R_5$ is equivalent to $S_1 S_4$.

Suppose there is an exterior arc $R_a S_b$ with ancestors $R_i R_j$ and $S_{i'} S_{j'}$. Then $R_i R_j$ is *subsumed* in $S_{i'} S_{j'}$, if for any $R_k S_{k'} \in I'$, $i < k < j$ implies $i' < k' < j'$, see Fig. 1, (B). If $R_{i_1} R_{j_1}$ is subsumed in $S_{i_2} S_{j_2}$ and *vice versa*, we call these arcs *equivalent*. A *zigzag*, is a subgraph containing two dependent interior arcs $R_{i_1} R_{j_1}$ and $S_{i_2} S_{j_2}$ neither one subsuming the other, see Fig. 2, (A).

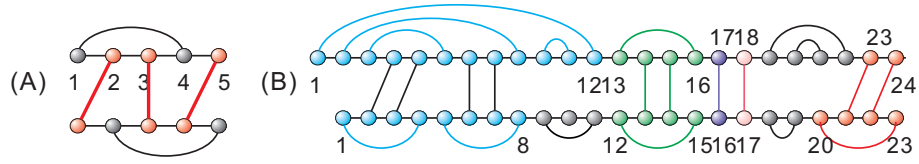


FIGURE 2. (A): A zigzag, generated by $R_2 S_1$, $R_3 S_3$ and $R_5 S_4$. (B): We partition the joint structure $J_{1,24;1,23}$ in segments and tight structures.

A *joint structure*, $J(R, S, I)$, is a zigzag-free pre-structure, see Fig. 2, (B). Joint structures are exactly the configurations that are considered in the maximum matching approach of [4], in the energy minimization algorithm of [1], and in the partition function approach of [2]. The subgraph of a joint structure $J(R, S, I)$ induced by a pair of subsequences $\{R_i, R_{i+1}, \dots, R_j\}$ and $\{S_h, S_{h+1}, \dots, S_\ell\}$ is denoted by $J_{i,j;h,\ell}$. In particular, $J(R, S, I) = J_{1,N;1,M}$. We say $R_a R_b(S_a S_b, R_a S_b) \in J_{i,j;h,\ell}$ if and only if $R_a R_b(S_a S_b, R_a S_b)$ is an edge of the graph $J_{i,j;h,\ell}$. Furthermore, $J_{i,j;h,\ell} \subset J_{a,b;c,d}$ if and only if $J_{i,j;h,\ell}$ is a subgraph of $J_{a,b;c,d}$ induced by $\{R_i, \dots, R_j\}$ and $\{S_h, \dots, S_\ell\}$.

We next define a *tight* structure (TS). Given a joint structure, $J_{a,b;c,d}$, its tight $J_{a',b';c',d'}$ is either a single exterior arc $R_{a'}S_{c'}$ (in the case $a' = b'$ and $c' = d'$), or the minimal block centered around the leftmost and rightmost exterior arcs α_l, α_r , (possibly being equal) and an interior arc subsuming both, i.e., $J_{a',b';c',d'}$ is tight in $J_{a,b;c,d}$ if it has either an arc $R_{a'}R_{b'}$ or $S_{c'}S_{d'}$ if $a' \neq b'$ or $c' \neq d'$.

More formally, let $J_{a',b';c',d'}$ be contained in $J_{a,b;c,d}$ with rightmost and leftmost exterior arc R_iS_j and $R_{i_0}S_{j_0}$ and let M be the set of R_iS_j -ancestors in $J_{a,b;c,d}$ with maximal length. Then $J_{a',b';c',d'}$ is tight in $J_{a,b;c,d}$ if

- (1) for $M = \emptyset$: $J_{a',b';c',d'} = \{R_iS_j\}$;
- (2) for $M = \{R_{i_1}R_{j_1}\}$: $J_{a',b';c',d'} = J_{i_1,j_1;c',j}$, where c' is the origin (left) of the S -ancestor of $R_{i_0}S_{j_0}$ with maximal length (or i_0 if there is none). The case $M = \{S_{r_1}S_{s_1}\}$ is analogous;
- (3) for $M = \{R_{i_1}R_{j_1}, S_{r_1}S_{s_1}\}$, suppose $R_{i_1}R_{j_1}$ subsumes $S_{r_1}S_{s_1}$. Then $J_{a',b';c',d'} = J_{i_1,j_1;x_1,s_1}$, where x_1 is the origin of the S -ancestor of $R_{i_0}S_{j_0}$ with maximal length (or i_0 if there is none). In particular, $J_{a',b';c',d'} = J_{i_1,j_1;r_1,s_1}$ when $R_{i_1}R_{j_1}$ is equivalent with $S_{r_1}S_{s_1}$. The case, where $S_{r_1}S_{s_1}$ subsumes $R_{i_1}R_{j_1}$ is analogous.

In the following, a TS is denoted by $J_{i,j;h,\ell}^T$. If $J_{a',b';c',d'}$ is tight in $J_{a,b;c,d}$, then we call $J_{a,b;c,d}$ its envelope. By construction, the notion of TS is depending on its envelope. There are only four basic types of TS:

- \circ : $\{R_iS_h\} = J_{i,j;h,\ell}^\circ$ and $i = j, h = \ell$;
- ∇ : $R_iR_j \in J_{i,j;h,\ell}^\nabla$ and $S_hS_\ell \notin J_{i,j;h,\ell}^\nabla$;
- \square : $\{R_iR_j, S_hS_\ell\} \in J_{i,j;h,\ell}^\square$;
- \triangle : $S_hS_\ell \in J_{i,j;h,\ell}^\triangle$ and $R_iR_j \notin J_{i,j;h,\ell}^\triangle$.

A *hybrid* structure, $J_{i_1,i_\ell;j_1,j_\ell}^{\text{Hy}}$, is a *maximal* sequence of intermolecular interior loops consisting of exterior arcs $(R_{i_1}S_{j_1}, \dots, R_{i_\ell}S_{j_\ell})$ where $R_{i_h}S_{j_h}$ is nested within $R_{i_{h+1}}S_{j_{h+1}}$ and where the internal segments $R[i_h + 1, i_{h+1} - 1]$ and $S[j_h + 1, j_{h+1} - 1]$ consist of single-stranded nucleotides only. That is, a hybrid is the maximal unbranched stem-loop formed by external arcs. Each hybrid thus forms a distinctive region of interaction between the two RNAs.

We call a joint structure *right-tight* (RTS), $J_{i,j;r,s}^{RT}$ in $J_{i_1,j_1;r_1,s_1}$ if its rightmost block is a $J_{i_1,j_1;r_1,s_1}$ -TS and *double-tight* (DTS), $J_{i,j;r,s}^{DT}$ in $J_{i_1,j_1;r_1,s_1}$ if both of its leftmost and its rightmost blocks are $J_{i_1,j_1;r_1,s_1}$ -TS's. In particular, we consider single interaction arcs as particular DTS.

1.2. Energy model. Let us review the energy model, implemented in `rip2`. The standard energy model for RNA folding [3] is consistent with the basic decomposition of secondary structure diagrams in the following sense: for secondary structures, we have

$$(1.1) \quad S \rightarrow .S \mid PS \mid P \quad \text{and} \quad P \rightarrow (S)$$

representing the cases that either the first base pair is unpaired or paired. Here S denotes an arbitrary structure, while P is secondary structure enclosed by a base pair. In fact, we use this decomposition to evaluate the secondary structure segments A and B in Fig. 7 of the main document.

The energy model, however, enforces a further refinement of the decomposition by distinguishing three different types of loops, for which energy contributions need to be computed by means of different rules: hairpin loops $P \rightarrow \text{Ha}$, interior loops (including bulges and stacked base pairs) $P \rightarrow \text{Int}$, and multi-branched loops: $P \rightarrow \text{M}$. These are now expanded further

$$(1.2) \quad \text{Ha} \rightarrow (h) \quad \text{Int} \rightarrow (i'Pi'') \quad \text{M} \rightarrow (M'M'')$$

where h , i' , i'' are the unpaired regions of the hairpin and interior loops. Multi-branch loops are further decomposed into components with a single branch M' and with multiple branches M'' for which the energy contributions are assumed to be additive. For completeness, we recall the productions $M' \rightarrow .M'|P$ and $M'' \rightarrow .M''|PM''|Pm$, where m is a stretch of unpaired nucleotides. The importance of this refined decomposition lies in the fact that the energy of each substructure can be obtained as a sum of the energies of the substructures associated with non-terminal symbols and an additional contribution that depends uniquely on the production and the terminals. The latter rules form the specific *energy parameters* [3].

The energy model, implemented in `rip2` (also in `rip1`) is an extension of the standard energy model of RNA secondary structures and recognizes the following loop-types:

- (1) *Hairpin-loop*: a hairpin loop $\text{Ha}_{i,j}$ has tabulated energies $G_{i,j}^{\text{Ha}}$ depending on their sequence and length.

- (2) *Interior-loop*: an interior loop $\text{Int}_{i_1, j_1; i_2, j_2}$ also have tabulated energies $G_{i_1, j_1; i_2, j_2}^{\text{Int}}$.
- (3) *Multi-loop*: a multi-loop M_{i_0, j_0} has energy $\alpha_1 + \alpha_2(t+1) + \alpha_3 c_2$, where $t = |E_{R[i_0, j_0]}^i|$ (“branching order”) inside $R[i_0, j_0]$ and c_2 is the number of isolated vertices contained in $R[i_0, j_0]$.
- (4) *Kissing-loop*: a kissing-loop K_{i_0, j_0} has energy $\beta_1 + \beta_2(t+1) + \beta_3 c_2$, where $t = |E_{R[i_0, j_0]}^i|$ and c_2 is the number of isolated vertices contained in $R[i_0, j_0]$, analogous to the parametrization of multiloops.
- (5) *Hybrid*: a hybrid $\text{Hy}_{i_1, i_\ell; j_1, j_\ell}$ has energy $G_{i_1, i_\ell; j_1, j_\ell}^{\text{Hy}} = \sigma_0 + \sigma \sum_{\theta} G_{i_\theta, i_{\theta+1}; j_\theta, j_{\theta+1}}^{\text{Int}}$, where a intermolecular interior loop formed by $R_{i_\theta} S_{j_\theta}$ and $R_{i_{\theta+1}} S_{j_{\theta+1}}$ is treated like an interior loop $\text{Int}_{i_\theta, j_\theta; i_{\theta+1}, j_{\theta+1}}$ with an affine scaling σ .

1.3. Structural components. In Figure 3 we display the twelve basic structural components: **A**, **B**: maximal secondary structure segments, $R[i, j]$ and $S[r, s]$, respectively; **C**: an arbitrary joint structure $J_{i, j; r, s}$; **D**: a right-tight structures $J_{i, j; r, s}^{RT}$; **E**: a double-tight structure $J_{i, j; r, s}^{DT}$; **F**: a tight structure having type ∇ , Δ or \square , respectively; **G**: a tight structure, $J_{i, j; r, s}^{\square}$, of type \square ; **H**: a tight structure, $J_{i, j; r, s}^{\nabla}$, of type ∇ ; **J**: a tight structure, $J_{i, j; r, s}^{\Delta}$, of type Δ ; **K**: exterior arc; **L**: isolated segment; **M**: pair of secondary segments, one of which containing at least one arc; **N**: hybrid structure $J_{i, j; h, \ell}^{\text{Hy}}$; **O**: substructure of a hybrid $J_{i, j; h, \ell}^{\text{h}}$ such that $R_i S_j$ and $R_h S_\ell$ are exterior arcs and $J_{i, j; h, \ell}^{\text{h}}$ itself is not a hybrid since it is not maximal.

2. CONSTRUCTION OF THE DECOMPOSITION TREES ACCORDING TO THE HYBRID-GRAMMAR

Procedure (a) [Block Decomposition]

input: a joint structure $\vartheta_0 = J_{i, j; h, \ell}$, which is neither a ϑ_0 -TS of type $\{\nabla, \Delta, \square\}$ nor a maximal secondary segment (MS).

output: a unique tree $T_a(\vartheta_0) = (V_a(T), E_a(T))$

Let $i \leq j^* \leq j+1$ and $R[j^*, j]$ be the ϑ_0 -MS contain j . In particular, $j^* = j+1$ in case of such an MS does not exist and $j^* = i$ if $R[i, j]$ itself is a MS. Analogously, we define $S[\ell^*, \ell]$. We construct the tree $T_a(\vartheta_0)$ recursively as follows:

initialization: $V_a(T) = \{\vartheta_0\}$ and $E_a(T) = \emptyset$.

(a1): in case of $j^* = j+1$ and $\ell^* = \ell+1$, i.e. ϑ_0 is RTS. Let $i-1 \leq i^* < j$ and $R[i, i^*]$ be the ϑ_0 -MS contain i and analogously define $S[h, h^*]$, where $h-1 \leq h^* < \ell$. Consider the number of ϑ_0 -TS



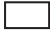









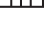

	A : maximal secondary structure segments $R[i, j]$;
	B : maximal secondary structure segments $S[r, s]$;
	C : arbitrary joint structure $J_{i,j;r,s}$
	D : right-tight structures $J_{i,j;r,s}^{RT}$
	E : double-tight structure $J_{i,j;r,s}^{DT}$;
	F : tight structure of type ∇ , Δ or \square ;
	G : type \square tight structure $J_{i,j;r,s}^{\square}$;
	H : type ∇ tight structure $J_{i,j;r,s}^{\nabla}$;
	J : type Δ tight structure $J_{i,j;r,s}^{\Delta}$;
	K : exterior arc;
	L : isolated segment;
	M : pair of secondary segments such that they are not isolated segments at the same time.
	N : hybrid structure $J_{i,j;h,\ell}^{Hy}$;
	O : substructure of a hybrid $J_{i,j;h,\ell}^h$ such that $R_i S_\ell$ and $R_h S_\ell$ are exterior arcs.

FIGURE 3. The panel displays the twelve basic types of structural components.

exist in $J_{i,j;h,\ell}^{RT}$, θ_1 , we have two cases. In case of $\theta = 1$, then ϑ_0 decomposes into $\vartheta_1 = R[i, i^*]$, $\vartheta_2 = S[h, h^*]$ and a ϑ_0 -TS $\vartheta_3 = J_{i^*+1,j;h^*+1,\ell}^{\{\nabla,\Delta,\square,\circ\}}$. Otherwise, ϑ_0 decomposes into $\vartheta_1 = R[i, i^*]$, $\vartheta_2 = S[h, h^*]$ and a ϑ_0 -DTS $\vartheta_3 = J_{i^*+1,j;h^*+1,\ell}^{DT}$.

Accordingly, we have

$$(2.1) \quad V_a(T) = V_a(T) \cup \{\vartheta_1, \vartheta_2, \vartheta_3\},$$

$$(2.2) \quad E_a(T) = E_a(T) \cup \{\vartheta_0\vartheta_1, \vartheta_0\vartheta_2, \vartheta_0\vartheta_3\}.$$

Furthermore, a ϑ_0 -DTS, $\vartheta_3 = J_{i^*+1,j;h^*+1,\ell}^{DT}$, depending on whether $J_{i^*+1,j;h^*+1,\ell}^{DT}$ is a hybrid, there are two cases. In case of $J_{i^*+1,j;h^*+1,\ell}^{DT} = J_{i^*+1,j;h^*+1,\ell}^{Hy}$, depending on whether $J_{i^*+1,j;h^*+1,\ell}^{Hy}$ is a single exterior arc, there are two subcases, in case of $J_{i^*+1,j;h^*+1,\ell}^{Hy} = R_j S_\ell$, nothing changes, otherwise let $R_{j^*} S_{\ell^*}$ be the exterior arc such that $R[j^*+1, j-1]$ and $S[\ell^{*+1}, \ell-1]$ are unpaired nucleotides. ϑ_3 decomposes into a substructure of hybrid, $\vartheta_4 = J_{i^*+1,j^*;h^*+1,\ell^*}^h$ and an exterior arc $\vartheta_5 = R_j S_\ell$. Accordingly, we obtain

$$(2.3) \quad V_a(T) = V_a(T) \cup \{\vartheta_4, \vartheta_5\},$$

$$(2.4) \quad E_a(T) = E_a(T) \cup \{\vartheta_3\vartheta_4, \vartheta_3\vartheta_5\}.$$

Furthermore, as a substructure of hybrid, $\vartheta_4 = J_{i^*+1,j^*;h^*+1,\ell^*}^h$ can be recursively decomposed into a smaller substructure of hybrid and an exterior arc from right to left.

Otherwise, in case of $J_{i^*+1,j;h^*+1,\ell}^{DT}$ is not a hybrid, depending on the type of the leftmost TS, $J_{i^*+1,j_1;h^*+1,\ell_1}^T$, we have two subcases. In case of $J_{i^*+1,j_1;h^*+1,\ell_1}^T$ is of type lies in $\{\nabla, \triangle, \square\}$, ϑ_3 decomposes into a ϑ_3 -TS, $\vartheta_6 = J_{i^*+1,j_1;h^*+1,\ell_1}^{\{\nabla, \triangle, \square\}}$ and a ϑ_3 -RTS $\vartheta_7 = J_{j_1+1,j;\ell_1+1,\ell}^{RT}$. Accordingly, we obtain

$$(2.5) \quad V_a(T) = V_a(T) \cup \{\vartheta_6, \vartheta_7\},$$

$$(2.6) \quad E_a(T) = E_a(T) \cup \{\vartheta_3\vartheta_6, \vartheta_3\vartheta_7\}.$$

Otherwise, in case of $J_{i^*+1,j_1;h^*+1,\ell_1}^T$ is of type \circ , ϑ_3 decomposes into a hybrid $\vartheta_8 = J_{i^*+1,j_2;h^*+1,\ell_2}^{Hy}$ and a ϑ_3 -RTS $\vartheta_9 = J_{j_2+1,j;\ell_2+1,\ell}^{RT}$. Accordingly, we have

$$(2.7) \quad V_a(T) = V_a(T) \cup \{\vartheta_8, \vartheta_9\},$$

$$(2.8) \quad E_a(T) = E_a(T) \cup \{\vartheta_3\vartheta_8, \vartheta_3\vartheta_9\}.$$

(a2) Otherwise, ϑ_0 decomposes into a RTS $\vartheta_3 = J_{i,j^*-1;h,\ell^*-1}^{RT}$ in ϑ_0 and two MS's $\vartheta_4 = R[j^*, j]$, $\vartheta_5 = S[\ell^*, \ell]$. Accordingly, we have

$$(2.9) \quad V_a(T) = V_a(T) \cup \{\vartheta_3, \vartheta_4, \vartheta_5\},$$

$$(2.10) \quad E_a(T) = E_a(T) \cup \{\vartheta_0\vartheta_3, \vartheta_0\vartheta_4, \vartheta_0\vartheta_5\}.$$

We iterate the process until all the leaves of $T_a(\vartheta_0)$ are either ϑ_0 -TS or ϑ_0 -MS.

Procedure (b): [Arc Removal]

input: a TS $\vartheta_0 = J_{i,j;h,\ell}$

output: a unique tree $T_b(\vartheta_0) = (V_b(T), E_b(T))$

initialization: $V_b(T) = \{\vartheta_0\}$ and $E_b(T) = \emptyset$.

We distinguish $J(i, j; h, \ell)$ by type:

○: do nothing.

□: ϑ_0 decomposes into $\vartheta_1 = R_i R_j$, $\vartheta_2 = R[i+1, i_1-1]$, $\vartheta_3 = J_{i_1, j_1; h, \ell}^{\{\square, \triangle\}}$ and $\vartheta_4 = R[j_1+1, j-1]$, which gives rise to

$$(2.11) \quad V_b(T) = V_a(T) \cup \{\vartheta_1, \vartheta_2, \vartheta_3, \vartheta_4\},$$

$$(2.12) \quad E_b(T) = E_a(T) \cup \{\vartheta_0\vartheta_1, \vartheta_0\vartheta_2, \vartheta_0\vartheta_3, \vartheta_0\vartheta_4\}.$$

▽: we consider the set of $J_{i+1, j-1; h, \ell}$ -tight structures, denoted by M . In case of $|M| = 1$, $J_{i+1, j-1; h, \ell}$ decompose into a sequence of a $J_{i+1, j-1; h, \ell}$ -tight structure $\vartheta_6 = J_{i+1, j-1; h, \ell}^{\{\nabla, \circ\}}$ and two $J_{i+1, j-1; h, \ell}$ -MS, $\vartheta_7 = R[i+1, i_1-1]$ and $\vartheta_8 = R[j_1+1, j-1]$, where $i \leq i_1 < j_1 \leq j$. Accordingly,

$$(2.13) \quad V_b(T) = V_a(T) \cup \{\vartheta_1, \vartheta_6, \vartheta_7, \vartheta_8\},$$

$$(2.14) \quad E_b(T) = E_a(T) \cup \{\vartheta_0\vartheta_1, \vartheta_0\vartheta_6, \vartheta_0\vartheta_7, \vartheta_0\vartheta_8\}.$$

In case of $|M| > 1$, $J_{i+1, j-1; h, \ell}$ decomposes into a sequence consisting of a DTS in $J_{i+1, j-1; h, \ell}$, denoted by $\vartheta_9 = J_{i+1, j-1; h, \ell}^{DT}$ and two $J_{i+1, j-1; h, \ell}$ -ms. $\vartheta_7 = R[i+1, i_1-1]$ and $\vartheta_8 = R[j_1+1, j-1]$, where $i \leq i_1 < j_1 \leq j$. Accordingly,

$$(2.15) \quad V_b(T) = V_a(T) \cup \{\vartheta_1, \vartheta_7, \vartheta_8, \vartheta_9\},$$

$$(2.16) \quad E_b(T) = E_a(T) \cup \{\vartheta_0\vartheta_1, \vartheta_0\vartheta_7, \vartheta_0\vartheta_8, \vartheta_0\vartheta_9\}.$$

△: analogous to type ▽ via symmetry.

Finally, we have the well-known secondary structure loop-decomposition

Procedure (c): [Secondary Structure]

input: a secondary structure $\vartheta_0 = R[i, j]$

output: a tree $T_c(\vartheta_0) = (V_c(T), E_c(T))$

initialization: $V_b(T) = \{\vartheta_0\}$ and $E_b(T) = \emptyset$.

We distinguish the following two cases:

(c1): in case of $R_i R_j \notin R[i, j]$, let \varnothing_a^b denote empty segment in which all the vertices are isolated. For $1 \leq j^* \leq j+1$, let $\varnothing_{j^*}^j$ be the maximal empty segment that contains R_j . In particular, if j is not isolated, we have $j^* = j+1$. Let $R^b(i_1, j^* - 1)$ denote the segment in which R_{i_1} is connected with $R_{j^* - 1}$. Then $R[i, j]$ decomposes as follows $R[i, j] = (\vartheta_1 = R[i, i_1 - 1], \vartheta_2 = R^b(i_1, j^* - 1), \vartheta_3 = \varnothing_{j^*}^j)$ and we set

$$(2.17) \quad V_c(T) = V_c(T) \cup \{\vartheta_1, \vartheta_2, \vartheta_3\},$$

$$(2.18) \quad E_c(T) = E_c(T) \cup \{\vartheta_0\vartheta_1, \vartheta_0\vartheta_2, \vartheta_0\vartheta_3\}.$$

(c2): in case of $R_i R_j \in R[i, j]$, i.e. for $R[i, j] = R^b(i, j)$, we have a decomposition into the pair $(\vartheta_4 = R_i R_j, \vartheta_5 = R[a+1, b-1])$. Accordingly, we have $V_c(T) = V_c(T) \cup \{\vartheta_4, \vartheta_5\}$ and $E_c(T) = E_c(T) \cup \{\vartheta_0\vartheta_4, \vartheta_0\vartheta_5\}$.

We iterate (c1) and (c2), until all the leaves in T are either isolated segments or single arcs.

For any joint structure, $J_{1,N;1,M}$, we can now construct a tree, with root $J_{1,N;1,M}$ and whose vertices are specific subgraphs of $J_{1,N;1,M}$. To be precise, let H be the graph rooted in $J_{1,N;1,M}$ defined inductively as follows: for the induction basis for fixed $J_{1,N;1,M}$ only one, Procedure (a), (b) or (c) applies. Procedure (a), (b) or (c) generates the (procedure-specific, nontrivial) subtrees, T_a , T_b and T_c . Suppose ϑ_{\dagger} is a leaf of T that has been constructed via Procedure (a), (b) or (c). As in case of the induction basis, each such leaf is input for exactly one procedure, which in turn generates a corresponding subtree. The construction imply that H itself is a tree. We denote this decomposition tree by $T_{J_{1,N;1,M}}$.

3. RECURRENCES

The computation of the partition function conceptually follows the logic of the McCaskill's approach for RNA secondary structures. The generalization of the computation of the base pairing probabilities, however, is less straight-forward. The reason is that base pairs in joint structures are not always the unique closing pairs of loop, hence base pairing probabilities cannot be identified directly with the probabilities of certain TS. Instead, one has to compute the pairing probabilities by explicitly "tracing back" all contributing joint structures.

The complete set of 4D-storage arrays and 2D-storage array for the partition function are displayed in the Tables 1-4.

TABLE 1. Tight structures, $Q_{i,j;r,s}^T$: 9 4D-arrays.

$Q_{\nabla,E}$	$Q_{\nabla,M}$	$Q_{\nabla,F}$
$Q_{\nabla,K}$	$Q_{\triangle,E}$	$Q_{\triangle,M}$
$Q_{\triangle,F}$	$Q_{\triangle,K}$	Q_{\square}

TABLE 2. Right-tight structures, $Q_{i,j;r,s}^{RT}$: 20 4D-arrays.

$Q_{RT,EEA}$	$Q_{RT,EEB}$	$Q_{RT,ME}$	$Q_{RT,EM}$	$Q_{RT,FE}$
$Q_{RT,EF}$	$Q_{RT,MM}$	$Q_{RT,MF}$	$Q_{RT,FM}$	$Q_{RT,FF}$
$Q_{RT,EKA}$	$Q_{RT,EKB}$	$Q_{RT,MK}$	$Q_{RT,FK}$	$Q_{RT,KEA}$
$Q_{RT,KEB}$	$Q_{RT,KM}$	$Q_{RT,KF}$	$Q_{RT,KKA}$	$Q_{RT,KKB}$

TABLE 3. Double-tight joint structures, $Q_{i,j;r,s}^{DT}$: 20 4D-matrices.

$Q_{DT,EEA}$	$Q_{DT,EEB}$	$Q_{DT,ME}$	$Q_{DT,EM}$	$Q_{DT,FE}$
$Q_{DT,EF}$	$Q_{DT,MM}$	$Q_{DT,MF}$	$Q_{DT,FM}$	$Q_{DT,FF}$
$Q_{DT,EKA}$	$Q_{DT,EKB}$	$Q_{DT,MK}$	$Q_{DT,FK}$	$Q_{DT,KEA}$
$Q_{DT,KEB}$	$Q_{DT,KM}$	$Q_{DT,KF}$	$Q_{DT,KKA}$	$Q_{DT,KKB}$

TABLE 4. Secondary segments: 8 2D-arrays.

Q^R	$Q^{R,b}$	$Q^{R,M}$	$Q^{R,F}$
Q^S	$Q^{S,b}$	$Q^{S,M}$	$Q^{S,F}$

The complete set of recursions comprises for tight structures $Q_{i,j;r,s}^T$, 9 4D-arrays, for right-tight joint structures $Q_{i,j;r,s}^{RT}$, 20 4D-arrays, for double-tight structures $Q_{i,j;r,s}^{DT}$, 20 4D-arrays, and 8 2D-arrays for secondary segments.

Structure-type	recurrence-formula (symbolic)
$J_{i,j;h,\ell}^{\nabla}$	Figure 6
$J_{i,j;h,\ell}^{\Delta}$	Figure 7
$J_{i,j;h,\ell}^{\square}$	Figure 8
$J_{i,j;h,\ell}^{DT}$	Figure 9
$J_{i,j;h,\ell}^{RT}$	Figure 10

4. MORE DATA

Given a RNA sequence, s , consider two hybrids in s , denoted by $A = J_{i_a, j_a; k_a, l_a}^{\text{Hy}}$ and $B = J_{i_b, j_b; k_b, l_b}^{\text{Hy}}$. Define the indicator function X_A as follows: $X_A(s) = 1$ if there is base pair $R_p S_q$ such that $i_a \leq p \leq j_a$, $k_a \leq q \leq l_a$ in the sampled structure s , and 0 otherwise. Analogously, we define $X_B(s)$.

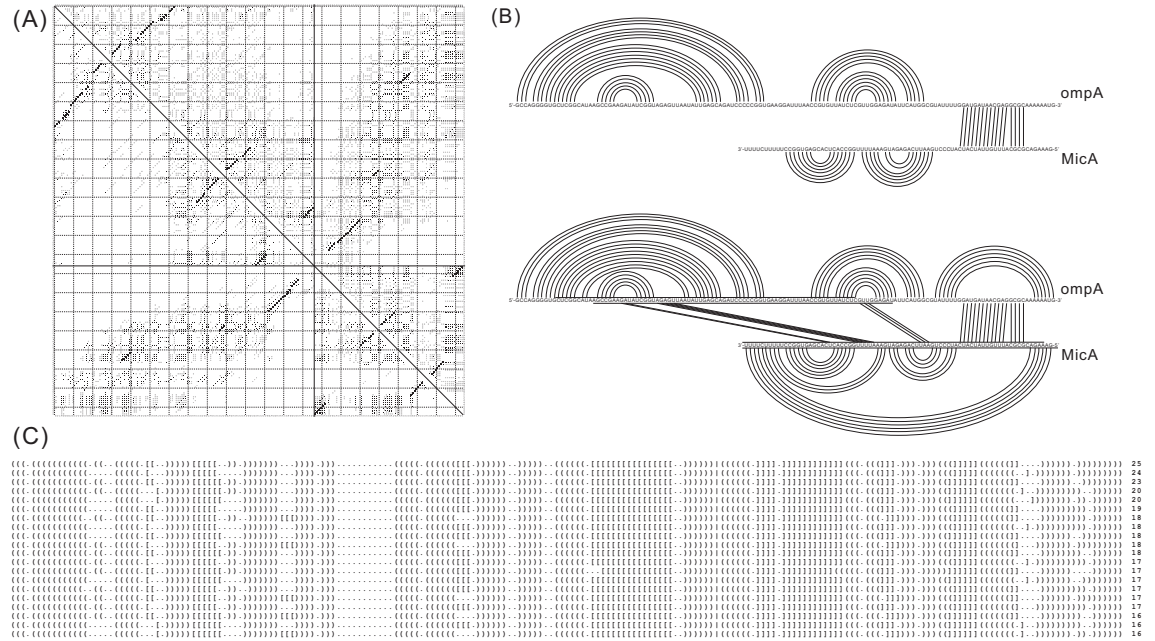


FIGURE 4. Interaction of *ompA-MicA*. (A) Base pairing probability matrix. The upper-right triangle shows the probabilities obtained from the exact backwards recursion, the lower-left triangle is the estimate from a sample of 500,000 structures obtained by stochastic backtracing, showing that the estimates converge quickly. (B) Comparison of the structure proposed in [5] and the `rip2` prediction. While the major stable hairpins agree and `rip2` correctly predicts the primary interaction region, `rip2` also identifies additional interaction regions that may stabilize the interaction. (C) Sampled joint structures (here the 20 most frequent ones) are represented as dot-bracket strings: $()$ and $[\]$ represent pairs of interior and exterior arc, respectively, while dots indicate unpaired bases. $|$ separates the two RNA sequences which are both written in $5' \rightarrow 3'$ direction.

TABLE 5. The top 5 hybrid-sampling frequencies for the interaction of *sodB-RyhB*.

$J_{i,j;h,\ell}^{\text{Hy}}$	$J_{52,60;45,53}^{\text{Hy}}$	$J_{15,17;11,13}^{\text{Hy}}$	$J_{38,47;26,35}^{\text{Hy}}$	$J_{72,75;69,72}^{\text{Hy}}$	$J_{77,78;79,80}^{\text{Hy}}$
$\mathbb{P}_{i,j;h,\ell}^{\text{Hy}}$	0.82230	0.53961	0.24124	0.17140	0.16124

 TABLE 6. The covariance of top 5 sampling-hybrids for the interaction of *sodB-RyhB*. We index the vertices such that R_1 is the 5' end of R and S_1 denotes the 3' end of S . For instance, $J_{52,60;45,53}^{\text{Hy}}$ is the hybrid formed by two intervals $[R_{52}, R_{60}]$ and $[S_{45}, S_{53}]$.

Covariance	1: $J_{52,60;45,53}^{\text{Hy}}$	2: $J_{15,17;11,13}^{\text{Hy}}$	3: $J_{38,47;26,35}^{\text{Hy}}$	4: $J_{72,75;69,72}^{\text{Hy}}$	5: $J_{77,78;79,80}^{\text{Hy}}$
1: $J_{52,60;45,53}^{\text{Hy}}$	0.0091644375	0.0000105125	0.00347623	0.001405585	-0.000682525
2: $J_{15,17;11,13}^{\text{Hy}}$	-	0.1851533775	0.007708706	0.001300787	-0.009122055
3: $J_{38,47;26,35}^{\text{Hy}}$	-	-	0.1983983344	0.1011387688	-0.032266132
4: $J_{72,75;69,72}^{\text{Hy}}$	-	-	-	0.2481354876	0.006675986
5: $J_{77,78;79,80}^{\text{Hy}}$	-	-	-	-	0.22201071

 TABLE 7. The top 5 hybrid-sampling frequencies for the interaction of *ompA-MicA*. We index the vertices such that R_1 is the 5' end of R and S_1 denotes the 3' end of S .

$J_{i,j;h,\ell}^{\text{Hy}}$	$J_{113,128;55,71}^{\text{Hy}}$	$J_{87,89;45,47}^{\text{Hy}}$	$J_{39,40;19,20}^{\text{Hy}}$	$J_{67,69;51,53}^{\text{Hy}}$	$J_{27,28;21,22}^{\text{Hy}}$
$\mathbb{P}_{i,j;h,\ell}^{\text{Hy}}$	0.61477	0.25157	0.20731	0.13927	0.12372

 TABLE 8. The covariance of top 5 sampling-hybrids for the interaction of *ompA-MicA*. We index the vertices such that R_1 is the 5' end of R and S_1 denotes the 3' end of S . For instance, $J_{113,128;55,71}^{\text{Hy}}$ is the hybrid formed by two intervals $[R_{113}, R_{128}]$ and $[S_{55}, S_{71}]$.

Covariance	1: $J_{113,128;55,71}^{\text{Hy}}$	2: $J_{87,89;45,47}^{\text{Hy}}$	3: $J_{39,40;19,20}^{\text{Hy}}$	4: $J_{67,69;51,53}^{\text{Hy}}$	5: $J_{27,28;21,22}^{\text{Hy}}$
1: $J_{113,128;55,71}^{\text{Hy}}$	0.0000299991	0.0000104406	0.0000066726	0.0000075426	0.0000069108
2: $J_{87,89;45,47}^{\text{Hy}}$	-	0.2269020796	0.0363833916	-0.0874991884	-0.0177998872
3: $J_{39,40;19,20}^{\text{Hy}}$	-	-	0.1729493436	-0.0483208364	-0.0512366712
4: $J_{67,69;51,53}^{\text{Hy}}$	-	-	-	0.1882079836	0.0243728888
5: $J_{27,28;21,22}^{\text{Hy}}$	-	-	-	-	0.1772942704

5. COMPUTATION OF THE PROBABILITIES

In contrast to the computation of the partition function “from the inside to the outside”, the computation of the base pairing probabilities (BPP) is obtained “from the outside to the inside”. Let $\mathbb{J}_{i,j;h,\ell}^{\xi, Y_1 Y_2 Y_3}$ be the set of substructures $J_{i,j;h,\ell} \subset J_{1,N;1,M}$ such that $J_{i,j;h,\ell}$ appears in $T_{1,N;1,M}$ as an interaction structure of type $\xi \in \{DT, RT, \nabla, \Delta, \square, \circ\}$ with loop-subtypes $Y_1, Y_2 \in \{M, K, F\}$ on the sub-intervals $R[i, j]$ and $S[h, \ell]$, $Y_3 \in \{A, B\}$. Let $\mathbb{P}_{i,j;h,\ell}^{\xi, Y_1 Y_2 Y_3}$ be the probability of $\mathbb{J}_{i,j;h,\ell}^{\xi, Y_1 Y_2 Y_3}$. For instance, $\mathbb{P}_{i,j;h,\ell}^{RT, MKA}$ is the sum over all the probabilities of substructures $J_{i,j;h,\ell} \in T_{1,N;1,M}$ such that $J_{i,j;h,\ell}$ is a right-tight structure of type rA and $R[i, j]$, $S[h, \ell]$ are enclosed by a multi-loop and kissing loop, respectively.

Algorithm 1 constructs recursively all 4D-arrays $\overline{P}_{i,i+j;r,r+s}^{\xi, Y_1 Y_2 Y_3}$. This is obtained via the corresponding arrays of partition functions over the respective subcomplexes and the quantities $P_{i,i+j;r,r+s}^{\xi, Y_1 Y_2 Y_3}$ from the outside to the inside. In other words Algorithm 1 facilitates the recursive translation of the 4D-arrays of partition functions into base pairing probabilities. By construction we have

$$(5.1) \quad \mathbb{P}_{i,i+j;r,r+s}^{\xi, Y_1 Y_2 Y_3} = P_{i,i+j;r,r+s}^{\xi, Y_1 Y_2 Y_3}.$$

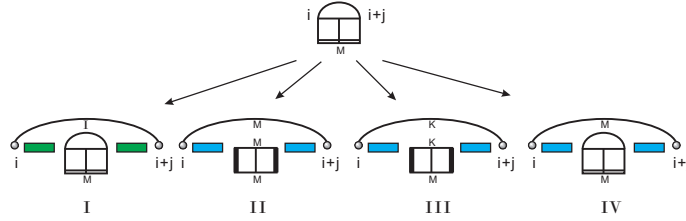


FIGURE 5. Further refinement: the four decompositions of $J_{i,j;r,s}^{\nabla, M}$ via Procedure (b). These cases correspond to the four contributions in Algorithm 1).

Algorithm 1 Case I to Case IV correspond to the four cases showed in Figure 5.

```

1:  $j \leftarrow \text{lengthR} - 1$ 
2: while  $j \geq 0$  do
3:   for  $i \leftarrow 1$  to  $\text{lengthR} - j$  do
4:      $s \leftarrow \text{lengthS} - 1$ 
5:     while  $s \geq 0$  do
6:       for  $r \leftarrow 1$  to  $\text{lengthS} - s$  do
7:          $\vdots$ 
8:         if  $Q_{i,i+j;r,r+s}^{\nabla,M} \neq 0$  then
9:           for  $h \leftarrow i + 1$  to  $i + j - 1$  do
10:            for  $\ell \leftarrow h$  to  $i + j - 1$  do
11:               $Q \leftarrow Q_{h,\ell;r,r+s}^{\nabla,M} \cdot e^{-G_{i,i+j;h,\ell}^{\text{int}}}$ 
12:               $P_{h,\ell;r,r+s}^{\nabla,M} \leftarrow P_{h,\ell;r,r+s}^{\nabla,M} + P_{i,i+j;r,r+s}^{\nabla,M} \cdot Q / Q_{i,i+j;r,r+s}^{\nabla,M}$  {Case I}
13:               $Q \leftarrow Q_{i+1,h-1}^{\text{R,M}} \cdot Q_{\ell+1,i+j-1}^{\text{R,M}} \cdot Q_{h,\ell;r,r+s}^{\nabla,M} \cdot \exp(-(\alpha_1 + 2\alpha_2)/RT)$ 
14:               $P_{h,\ell;r,r+s}^{\nabla,M} \leftarrow P_{h,\ell;r,r+s}^{\nabla,M} + P_{i,i+j;r,r+s}^{\nabla,M} \cdot Q / Q_{i,i+j;r,r+s}^{\nabla,M}$ 
15:               $P_{i+1,h-1}^{\text{R,M}} \leftarrow P_{i+1,h-1}^{\text{R,M}} + P_{i,i+j;r,r+s}^{\nabla,M} \cdot Q / Q_{i,i+j;r,r+s}^{\nabla,M}$ 
16:               $P_{\ell+1,i+j-1}^{\text{R,M}} \leftarrow P_{\ell+1,i+j-1}^{\text{R,M}} + P_{i,i+j;r,r+s}^{\nabla,M} \cdot Q / Q_{i,i+j;r,r+s}^{\nabla,M}$  {Case II}
17:               $Q \leftarrow Q_{i+1,h-1}^{\text{R,M}} \cdot Q_{\ell+1,i+j-1}^{\text{R,M}} \cdot Q_{h,\ell;r,r+s}^{\text{DT,MM}} \cdot \exp(-(\alpha_1 + \alpha_2)/RT)$ 
18:               $P_{h,\ell;r,r+s}^{\text{DT,MM}} \leftarrow P_{h,\ell;r,r+s}^{\text{DT,MM}} + P_{i,i+j;r,r+s}^{\nabla,M} \cdot Q / Q_{i,i+j;r,r+s}^{\nabla,M}$ 
19:               $P_{i+1,h-1}^{\text{R,M}} \leftarrow P_{i+1,h-1}^{\text{R,M}} + P_{i,i+j;r,r+s}^{\nabla,M} \cdot Q / Q_{i,i+j;r,r+s}^{\nabla,M}$ 
20:               $P_{\ell+1,i+j-1}^{\text{R,M}} \leftarrow P_{\ell+1,i+j-1}^{\text{R,M}} + P_{i,i+j;r,r+s}^{\nabla,M} \cdot Q / Q_{i,i+j;r,r+s}^{\nabla,M}$  {Case III}
21:               $Q \leftarrow Q_{i+1,h-1}^{\text{R,F}} \cdot Q_{\ell+1,i+j-1}^{\text{R,F}} \cdot Q_{h,\ell;r,r+s}^{\text{DT,KM}} \cdot \exp(-(\beta_1 + \beta_2)/RT)$ 
22:               $P_{h,\ell;r,r+s}^{\text{DT,KM}} \leftarrow P_{h,\ell;r,r+s}^{\text{DT,KM}} + P_{i,i+j;r,r+s}^{\nabla,M} \cdot Q / Q_{i,i+j;r,r+s}^{\nabla,M}$ 
23:               $P_{i+1,h-1}^{\text{R,F}} \leftarrow P_{i+1,h-1}^{\text{R,F}} + P_{i,i+j;r,r+s}^{\nabla,M} \cdot Q / Q_{i,i+j;r,r+s}^{\nabla,M}$ 
24:               $P_{\ell+1,i+j-1}^{\text{R,F}} \leftarrow P_{\ell+1,i+j-1}^{\text{R,F}} + P_{i,i+j;r,r+s}^{\nabla,M} \cdot Q / Q_{i,i+j;r,r+s}^{\nabla,M}$  {Case IV}
25:            end for
26:          end for
27:         $\vdots$ 
28:      end for
29:       $s \leftarrow s - 1$ 
30:    end while
31:  end for
32:  $j \leftarrow j - 1$ 
end while

```

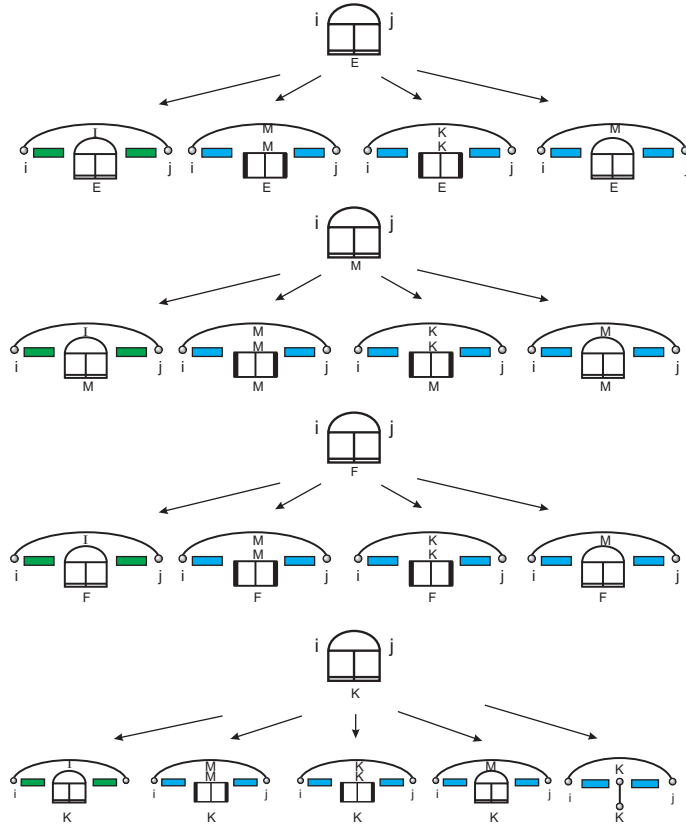


FIGURE 6. Decomposition for $J_{i,j}^{\nabla}$.

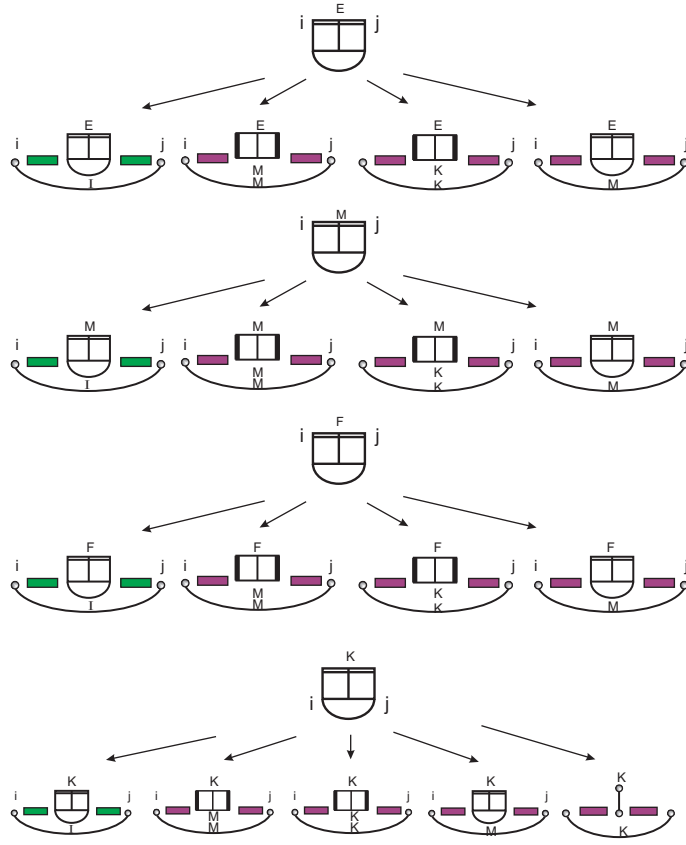


FIGURE 7. Decomposition for $J_{i,j;h,\ell}^{\Delta}$.

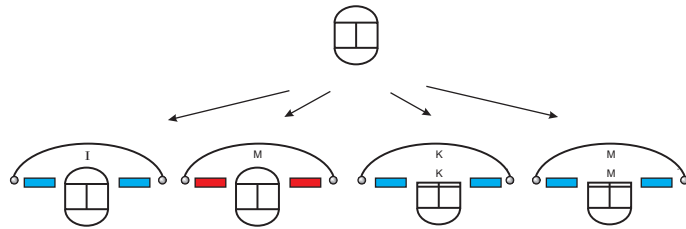


FIGURE 8. Decomposition for $J_{i,j;h,\ell}^{\square}$.

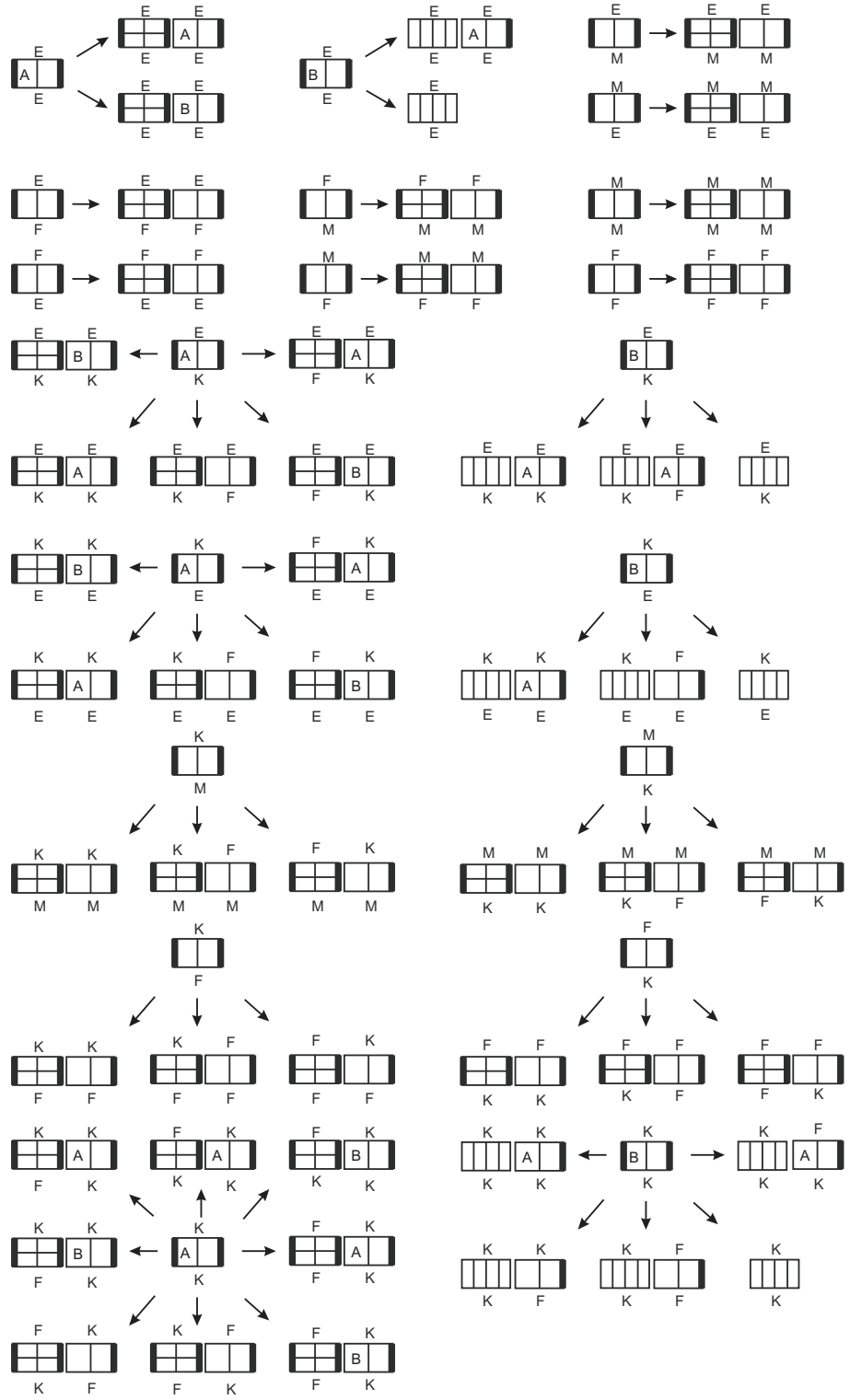


FIGURE 9. Decomposition for $J_{i,j;h,\ell}^{DT}$.

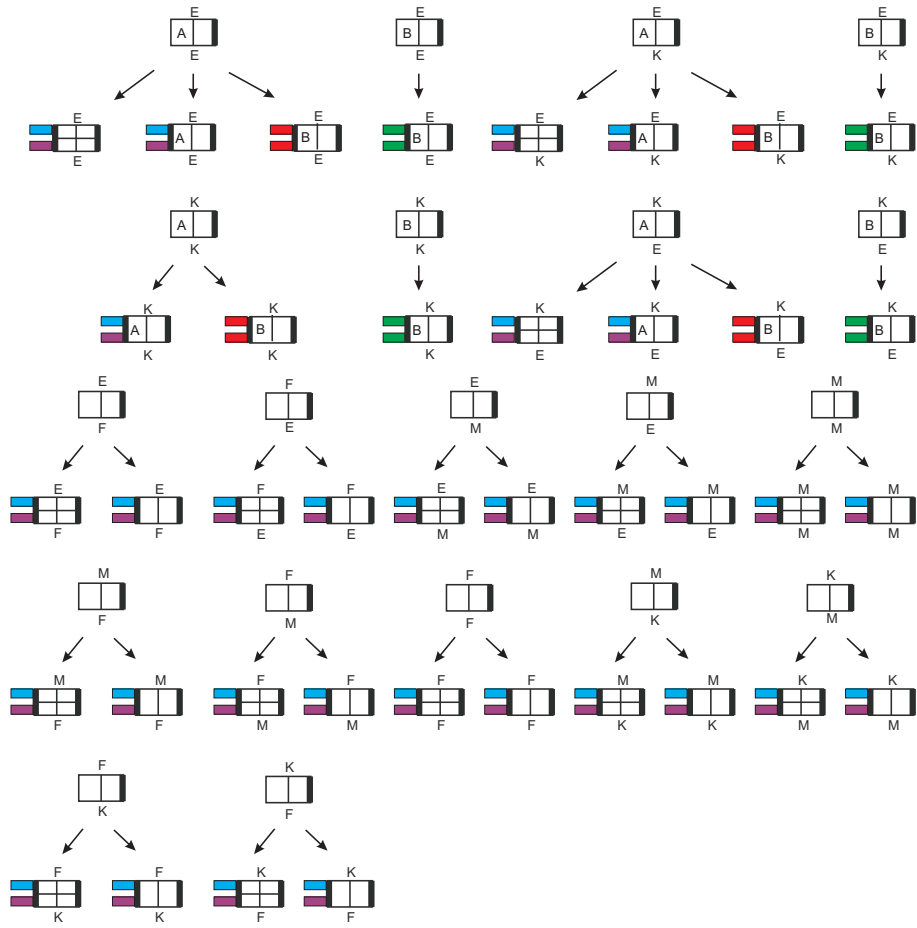


FIGURE 10. Decomposition for $J_{i,j;h,\ell}^{RT}$.

6. CONTRASTING THE **rip1**- AND **rip2**-GRAMMARS

Firstly, it is clear that the base pairing probabilities derived in **rip1** are not suited to characterize hybrid loops, since the probabilities of exterior arcs in hybrids can be strongly correlated. Similarly, the probabilities of blocks cannot be derived from base pair probabilities.

Secondly, as for using the probabilities of blocks considered in **rip1**, let us consider again the *sodB-RhyB* RNA-RNA interaction. Now we contrast $\pi_{i,k}$ -values based on the hybrids of the **rip2**-grammar and the various block-types available in the **rip1**-grammar. Since for neither DTS, RTS nor TS the quantities $\pi_{i,k}$ are sampling probabilities, we normalize the entries according to $0 \leq \pi_{i,k} \leq 1$. We denote $\pi_{i,k}[\text{Hy}] = \pi_{i,k}$ and these normalized coefficients by $\pi_{i,k}[\text{DTS}]$, $\pi_{i,k}[\text{RTS}]$ and $\pi_{i,k}[\text{TS}]$. In Fig. 11, we illustrate clearly that neither DTS's (**B**), nor RTS's (**C**) or TS's (**D**) can characterize the interaction regions adequately.

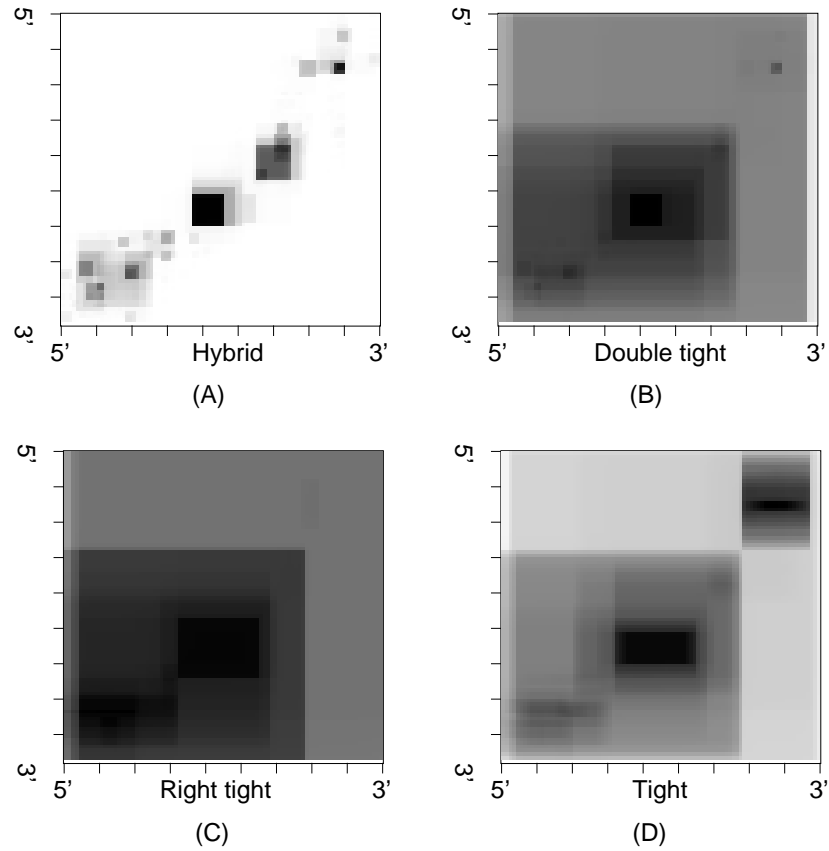


FIGURE 11. Contrasting the *rip1*- and *rip2*-grammars via the *sodB-RhyB* RNA-RNA interaction. We display $\pi_{i,k}[\text{Hy}]$ (A), $\pi_{i,k}[\text{DTS}]$ (B), $\pi_{i,k}[\text{RTS}]$ (C) and $\pi_{i,k}[\text{TS}]$ (D). Note that only $\pi_{i,k}[\text{Hy}]$ -terms are probabilities. The figure shows that only the hybrid-blocks of the *rip2*-grammar identify the two hybridization regions in the middle of the molecules and a diffuse contact area at the 3' end of *sodB*. The grayscale show the probabilities $\pi_{i,k}[\text{Hy}]$ and the normalized quantities $\pi_{i,k}[\text{DTS}]$, $\pi_{i,k}[\text{RTS}]$ and $\pi_{i,k}[\text{TS}]$. Tick marks indicate every 10th nucleotide.

REFERENCES

- [1] C. Alkan, E. Karakoc, J.H. Nadeau, S.C. Sahinalp, and K.Z. Zhang. RNA-RNA interaction prediction and antisense RNA target search. *J. Comput. Biol.*, 13:267–282, 2006.
- [2] H. Chitsaz, R. Salari, S.C. Sahinalp, and R. Backofen. A partition function algorithm for interacting nucleic acid strands. *Bioinformatics*, 25:i365–i373, 2009.
- [3] D. Mathews, J. Sabina, M. Zuker, and D.H. Turner. Expanded sequence dependence of thermodynamic parameters improves prediction of RNA secondary structure. *J. Mol. Biol.*, 288:911–940, 1999.
- [4] D.D. Pervouchine. IRIS: Intermolecular RNA interaction search. *Proc. Genome Informatics*, 15:92–101, 2004.
- [5] K.I. Udekwi, F. Darfeuille, J. Vogel, J. Reimegård, E. Holmqvist, and E. G. H. Wagner. Hfq-dependent regulation of OmpA synthesis is mediated by an antisense RNA. *Genes Dev.*, 19:2355–2366, 2005.

¹CENTER FOR COMBINATORICS, LPMC-TJKLC, NANKAI UNIVERSITY TIANJIN 300071, P.R. CHINA, ²COLLEGE OF LIFE SCIENCE, NANKAI UNIVERSITY TIANJIN 300071, P.R. CHINA, ³BIOINFORMATICS GROUP, DEPARTMENT OF COMPUTER SCIENCE, AND INTERDISCIPLINARY CENTER FOR BIOINFORMATICS, UNIVERSITY OF LEIPZIG, HÄRTELSTRASSE 16-18, D-04107 LEIPZIG, GERMANY., ⁴RNOMICS GROUP, FRAUNHOFER INSTITUT FOR CELL THERAPY AND IMMUNOLOGY, PERLICKSTRASSE 1, D-04103 LEIPZIG, GERMANY, ⁵INST. F. THEORETICAL CHEMISTRY, UNIVERSITY OF VIENNA, WÄHRINGERSTRASSE 17, A-1090 VIENNA, AUSTRIA, ⁶THE SANTA FE INSTITUTE, 1399 HYDE PARK RD., SANTA FE, NEW MEXICO

E-mail address: `duck@santafe.edu`